PAPER

Numerical investigation of hydrogen isotope retention by an yttrium pebble-bed from flowing liquid lithium

IOP Publishing | International Atomic Energy Agency Nuclear Fusion

Nucl. Fusion **60** (2020) 106017 (16pp) https://doi.org/10.1088/1741-4326/aba672

Numerical investigation of hydrogen isotope retention by an yttrium pebble-bed from flowing liquid lithium

S.J. Hendricks, E. Carella, C. Moreno and J. Molla

Ciemat, Av. Complutense, 40, 28040 Madrid, Spain

E-mail: sebastian.hendricks@ciemat.es

Received 30 April 2020, revised 15 June 2020
Accepted for publication 15 July 2020
Published 7 September 2020

Abstract

Ensuring a secure and reliable execution of the International Fusion Materials Irradiation Facility (IFMIF) and the DEMO-Oriented Neutron Source (DONES) requires their liquid lithium loops to be purified from hydrogen isotopes which are generated during operation. For this purpose, an yttrium pebble-bed will serve as a hydrogen hot trap. Former intentions to predict the retention behavior of an yttrium pebble-bed are based on the consideration of the trap as a black box with a predetermined trap efficiency. Disregarding the internal physical mechanisms of the gettering process these models are built on simplified assumptions and should be extended to allow reliable trap designs for IFMIF/DONES. Therefore, a detailed numerical model describing the hydrogen transport from flowing liquid lithium into an yttrium pebble-bed has been developed from scratch within the scope of this work. It enables simulating the hydrogen retention process into an arbitrarily dimensioned getter bed for the low concentration regime by solving a system of differential equations with a finite-difference approach. The model is used to calculate the time evolution of the hydrogen concentrations in a simplified loop system which is connected in line with an yttrium pebble-bed. Special focus is placed on the observation of a case relevant for IFMIF/DONES considering a constant generation of tritium in the loop. Simulation results reveal that the trap efficiency decreases with time and that lower system temperatures significantly improve the trap efficiency. It is found that for heavier pebble-beds the tritium inventory build-up in the lithium is slowed down more efficiently. These findings are of great importance for the design of the hot traps for IFMIF/DONES. To demonstrate the reliability of the model experimental data of a previous deuterium retention experiment are successfully reproduced.

Keywords: IFMIF, DONES, tritium modelling, hydrogen hot trap, liquid lithium, yttrium getter

(Some figures may appear in colour only in the online journal)

1. Introduction

Investigating the effects of high-energy neutron irradiation on fusion relevant materials is essential for the realization of future fusion power plants. The International Fusion Materials Irradiation Facility (IFMIF) and its reduced version the DEMO-Oriented Neutron Source (DONES) are designed for this purpose [1]. In both devices an accelerated high-energy deuterium beam collides with a liquid lithium target thus producing neutrons with energies similar to those expected at the first wall of a nuclear fusion reactor [2]. The liquid lithium flows through a loop system where due to the occurring nuclear reactions and residual deuterium deposition hydrogen isotopes are generated in a continuous manner. This leads to a linearly rising inventory of dissolved protium, deuterium and tritium in the loop. Due to corrosion between the lithium and the structural material of the loop further non-metallic impurities accumulate in the liquid lithium such as nitrogen, oxygen and

carbon. All mentioned impurities and especially the inventory build-up of radioactive tritium are a threat for the plants safety and chemical stability. Hence, it needs to be ensured that their concentrations are kept below certain concentration limits. For this purpose the liquid lithium loop of IFMIF/DONES will be connected in parallel to a purification side loop system. The purification side loop consists of an impurity monitoring loop and an impurity control system which are connected in parallel to the main loop. To remove the corrosion-related non-metallic impurities a cold trap forms the first unit of the impurity control system. Connected in line with the cold trap an yttrium pebble-bed will serve as a hydrogen isotope hot trap [3]. Yttrium has a much higher solubility of hydrogen isotopes than lithium. This causes a transport of hydrogen isotopes into the pebbles which is driven by the laws of diffusion and the imbalance of the chemical potentials in the two systems. The design and operation of the hot trap will be mainly determined by the IFMIF/DONES safety regulations that require the tritium inventory in the lithium as well as in the yttrium to be kept below 0.3g [4]. To ensure the fulfillment of the safety requirements it is essential to theoretically determine the most reasonable trap geometry, pebble-bed mass and pebble diameter for a certain system temperature. In former theoretical studies the retention behavior of an yttrium pebble-bed was estimated, regarding the trap as a black box with an either constant or concentration-dependent retention efficiency [5]. However, models based on such simplified considerations do not allow reproducing or explaining experimental data with an accuracy that would be sufficient for a reliable trap design. Therefore, a detailed numerical model describing the hydrogen transport from flowing liquid lithium into a bed of spherical yttrium pebbles is essential and has been developed from scratch within the scope of this work. In the model the governing physical processes are represented by a system of coupled algebraic and differential equations. Since an exact analytical calculation of the temporal evolution of the system is not possible the differential equation solver and non-causal programming software EcosimPro is used as a numerical simulate tool [6, 7]. EcosimPro allows object-orientated programming, thus enabling a facilitated numerical calculation of the time evolution of hydrogen isotope concentrations and particle fluxes at numerous discrete locations in the described system. However, the reliability of the theoretical model is highly dependent on the accuracy of several material and flow-specific experimental coefficients. Precisely measured temperature dependencies of the Sieverts' constant and the diffusion coefficient of hydrogen isotopes in lithium and yttrium as well as the mass transfer coefficient between a fluid and a solid pebble-bed are essential for the model to produce trustful results. For its validation, the developed numerical model is used to simulate the outcome of a deuterium retention experiment performed by Y. Yamasaki *et al* [5]. Good accordance between simulation results and the experimental data will demonstrate the accuracy of the simulation and thus create confidence to use this numerical model for the design of the hydrogen hot traps of IFMIF/DONES. In the following paragraphs the term *hydrogen* (H) will be used as a unified expression for all three hydrogen isotopes protium (^{1}H), deuterium (^{2}H) and tritium (^{3}H).

2. Numerical model

To simulate the behavior of an arbitrarily dimensioned yttrium pebble-bed in contact with hydrogen-loaded flowing liquid lithium a numerical model has been developed and is presented in the following paragraphs. In our model the hydrogen hot trap is considered as a cylindrical hollow container with an entrance and an exit port located at the top and the bottom side of the cylinder. The container is densely filled with yttrium pebbles of radius r_{peb}, diameter d_{peb} and a surface of S_{peb}. The volume of the trap cylinder is fixed through the relation $V_{\mathrm{trap}} = V_{\mathrm{Y}}/(1-\epsilon)$ where V_{Y} is the total volume occupied by the yttrium pebbles and ε the void fraction of the pebble-bed. For the qualification of the performance of the trap two quantities are defined. That is the trap efficiency

$$\mu_{\mathrm{trap}} = \frac{C_{\mathrm{Li,in}} - C_{\mathrm{Li,out}}}{C_{\mathrm{Li,in}}}, \tag{1}$$

where $C_{\mathrm{Li,in}}$ is the hydrogen concentration in the lithium at the entrance of the trap and $C_{\mathrm{Li,out}}$ the hydrogen concentration in the lithium at the exit of the trap. The second defined quantity is the hydrogen retention rate of the pebble-bed which stands for the number of absorbed hydrogen isotopes per second. In the developed numerical model of the hydrogen hot trap the total hydrogen retention rate of the yttrium pebble-bed $\dot{n}_{\mathrm{trap}}(t)$ is calculated as the sum of the retention rates of all yttrium pebbles. The time evolving retention rate of a single yttrium pebble $\dot{n}_{\mathrm{peb}}(t)$ can be calculated by

$$\dot{n}_{\mathrm{peb}}(t) = J_{\mathrm{ret}}(t) \cdot S_{\mathrm{peb}} = J_{\mathrm{ret}}(t) \cdot \pi d_{\mathrm{peb}}^2, \tag{2}$$

where $J_{\mathrm{ret}}(t)$ is the hydrogen retention flux from the lithium into the yttrium pebble. As we will see later the retention flux is dependent on the hydrogen concentration in the lithium at the interface between yttrium and lithium. Since the concentration varies along the longitudinal z-axis of the cylindrical trap container the total retention rate is being calculated integrating over the retention fluxes of all pebbles. For a trap container with length l_{trap} that contains a number of $\#_{\mathrm{peb}}$ yttrium pebbles we calculate

$$\dot{n}_{\mathrm{trap}}(t) = \#_{\mathrm{peb}} \cdot \frac{\pi d_{\mathrm{peb}}^2}{l_{\mathrm{trap}}} \int_0^{l_{\mathrm{trap}}} J_{\mathrm{ret}}(z,t)\,\mathrm{d}z\,. \tag{3}$$

In the lithium (Li) as well as in the yttrium (Y), hydrogen isotopes are transported by the diffusion process. According to Fick's first law the diffusion flux is proportional to the concentration gradient of hydrogen isotopes in the yttrium pebbles in radial direction

$$J_{\mathrm{dif,Y}}(r,z,t) = -D_{\mathrm{Y}} \frac{\partial C_{\mathrm{Y}}(r,z,t)}{\partial r}\,. \tag{4}$$

At the surface of the yttrium pebbles the hydrogen diffusion flux $J_{\mathrm{dif,Y}}(r = r_{\mathrm{peb}}, z, t)$ is equal to the hydrogen retention flux

$$J_{\mathrm{ret}}(z,t) = J_{\mathrm{dif,Y}}(r = r_{\mathrm{peb}}, z, t)\,. \tag{5}$$

The proportionality constant D_{Y} is the diffusion coefficient of hydrogen isotopes in yttrium. The interstitial atomic diffusion

Table 1. Temperature dependent diffusion coefficients of hydrogen in yttrium and lithium that are found in the literature. Error margins are indicated in case they were reported by the respective reference. The considered significant digits of the presented values are assumed from the respective reference taking into account unit conversions. If error margins are given the considered significant digits are adapted to the reported error. Diffusion relations printed in bold are those which are chosen to be used for the calculations performed in this work.

Diffusion coefficient $[\mathrm{m^2 s^{-1}}]$	Temperature range	References
$\boldsymbol{D_{\mathrm{Y},^1\mathrm{H}} = 1.3 \times 10^{-8} \cdot \exp\left(\frac{-4.2\times10^4 \frac{\mathrm{J}}{\mathrm{mol\cdot K}}}{R_{\mathrm{gas}} T}\right)}$	**470 °C – 850 °C**	**[10] (Refers to [11])**
$D_{\mathrm{Y},^1\mathrm{H}} = 300 \times 10^{-4} \cdot \exp\left(\frac{-16.0\times10^4 \frac{\mathrm{J}}{\mathrm{mol\cdot K}}}{R_{\mathrm{gas}} T}\right)$	687°C – 887°C	[12] (Measured)
$D_{\mathrm{Y},^1\mathrm{H}}\,(\pm 20\%) = 3.8 \times 10^{-7} \cdot \exp\left(\frac{-4.6\times10^4 \frac{\mathrm{J}}{\mathrm{mol\cdot K}}}{R_{\mathrm{gas}} T}\right)$	400°C – 1100°C	[13] (Calculated using [14–16])
$\boldsymbol{\log D_{\mathrm{Li},^3\mathrm{H}} = -8.562 + 1.737 \log T - \frac{110}{T}}$	**367 °C – 727 °C**	**[17] (Measured)**
$\log D_{\mathrm{Li},^1\mathrm{H}}\,(\pm 18\%) = -9.04 + 1.74 \log T - \frac{110}{T}$	615°C – 905°C	[13] (Calculated using [18, 19])
$D_{\mathrm{Li},^1\mathrm{H}} = 1.3 \pm 0.1 \times 10^{-3} \cdot \exp\left(\frac{-10.5\pm0.8\times10^4 \frac{\mathrm{J}}{\mathrm{mol\cdot K}}}{R_{\mathrm{gas}} T}\right)$	615°C – 905°C	[18] (Measured)
$D_{\mathrm{Li},^1\mathrm{H}} = 1.38 \cdot \exp\left(\frac{-16.2\times10^4 \frac{\mathrm{J}}{\mathrm{mol\cdot K}}}{R_{\mathrm{gas}} T}\right)$	500°C – 650°C	[20] (Measured)

coefficient of hydrogen isotopes in metals follows an Arrhenius type temperature dependence [8]

$$D = D_0 \cdot \exp\left(\frac{E_\mathrm{d}}{R_\mathrm{gas} T}\right) \qquad \left[\mathrm{m^2 s^{-1}}\right], \tag{6}$$

with D_0 being a pre-exponential factor and E_d the activation energy of diffusion. The constant R_gas labels the ideal gas constant given in $[\mathrm{J\ mol^{-1} K^{-1}}]$. For our calculation we focus on a temperature region between 250°C and 325°C since this is the proposed operation temperature region of the impurity control system of the DONES liquid lithium loop [9]. As we will see later on, higher temperatures lead to a lower trap efficiency.

In several previous experimental campaigns the temperature dependence of the diffusion coefficient of hydrogen isotopes in yttrium could be determined. The measurements were done applying different methods and covering different temperature intervals. A list of determined diffusion coefficient relations found in the literature can be seen in table 1. When plotting the different diffusion coefficients in yttrium against temperature applying each relation from table 1 it becomes apparent that they lead to highly different temperature dependencies. Especially towards low temperatures, the diffusion values produced by the three relations differ by several orders of magnitude. This gives rise to the assumption that at low temperatures the inaccuracy of all determined relations is relatively high. In the numerical model presented in this article we choose to implement the diffusion relation determined by J.B. Talbot *et al* [10]. The decision is based on the fact that the temperature interval in which the diffusion values were determined is closer to the temperature region of interest in comparison to the measurements performed by P.W. Fisher *et al* [12]. For the determination of the diffusion coefficient J.B. Talbot *et al* used the data set of only one experimental campaign in which the diffusion coefficient was determined for a high number of temperature values [11]. In contrast, R.E. Buxbaum *et al* used the data sets of three different experiments with a very low number of different temperature steps each [13]. Due to this fact we evaluated the diffusion relation of

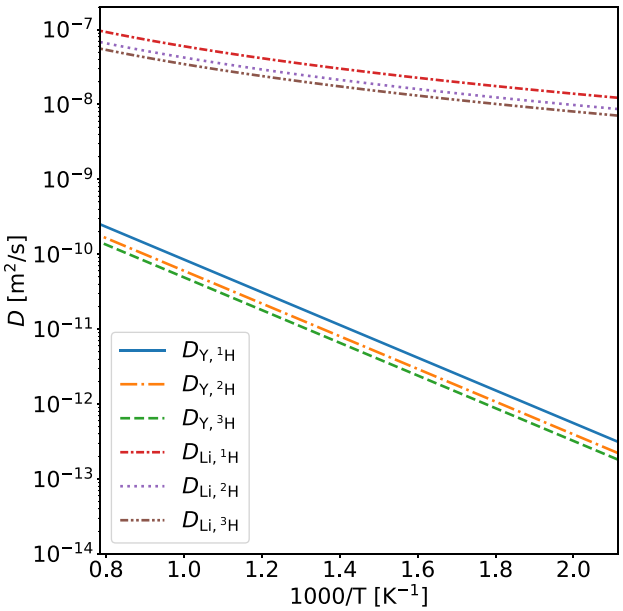

Figure 1. Temperature dependence of the diffusion coefficients for different hydrogen isotopes in yttrium and lithium determined by J.B. Talbot *et al* [10] and H. Moriyama *et al* [17].

J.B. Talbot *et al* to be most reliable for our application. The diffusion coefficients of deuterium and tritium in yttrium can be estimated through the isotope effect of hydrogen isotope diffusion in metal [21]

$$\frac{D_{\mathrm{Y},^1\mathrm{H}}}{D_{\mathrm{Y},^3\mathrm{H}}} = \sqrt{\frac{M_{^3\mathrm{H}}}{M_{^1\mathrm{H}}}} \;\&\; \frac{D_{\mathrm{Y},^1\mathrm{H}}}{D_{\mathrm{Y},^2\mathrm{H}}} = \sqrt{\frac{M_{^2\mathrm{H}}}{M_{^1\mathrm{H}}}} \;\&\; \frac{D_{\mathrm{Y},^2\mathrm{H}}}{D_{\mathrm{Y},^3\mathrm{H}}} = \sqrt{\frac{M_{^3\mathrm{H}}}{M_{^2\mathrm{H}}}}, \tag{7}$$

where M_H marks the molar mass of the corresponding hydrogen isotope. By applying these relations the diffusion coefficients of protium, deuterium and tritium in yttrium are plotted in figure 1. It appears that with rising temperature the diffusivity increases.

The time evolving concentration gradient $\partial_\mathrm{r} C_\mathrm{Y}(r,z,t)$ along the radial direction of a pebble is determined by Fick's second

law in spherical coordinates, given by

$$\frac{\partial C_{\mathrm{Y}}(r,z,t)}{\partial t} = \frac{D_{\mathrm{Y}}}{r^2}\frac{\partial}{\partial r}\left[r^2\frac{\partial C_{\mathrm{Y}}(r,z,t)}{\partial r}\right] = -\frac{\partial J_{\mathrm{dif,Y}}(r,z,t)}{\partial r}. \tag{8}$$

Due to the radial symmetry of the yttrium pebbles the concentration gradient at the center of a pebble is always zero. This forms a Neumann boundary condition

$$\frac{\partial C_{\mathrm{Y}}(r=0,z,t)}{\partial r} = 0. \tag{9}$$

For the description of the boundary condition at the interface between an yttrium pebble and the lithium it is important to define the thermodynamic regime of the yttrium-lithium-hydrogen system which we consider for this study. The presented model is based on the assumption that no yttrium oxides (Y_2O_3) are present in the system. An yttrium oxide layer formed around the pebble surfaces would drastically slow down the retention process [22].

The phase diagram of the yttrium-hydrogen (Y-H) binary system (see references [23–26]) reveals that within the temperature region of interest (250°C to 325°C) for low concentrations of approximately

$$C_{\mathrm{Y}_\alpha} < 27\mathrm{at}\% \mathrel{\widehat{=}} 1.9\times10^4\mathrm{mol\,m^{-3}} \tag{10}$$

the Y-H solution occurs in a single hexagonal-close-packed α-Y phase in which the hydrogen isotopes are distributed on tetrahedral interstitial sites without changing the structure of the metal lattice. For greater concentrations the β-phase begins to form. At a concentration of about

$$C_{\mathrm{Y}_\beta} \approx 65\mathrm{at}\% \mathrel{\widehat{=}} 9.3\times10^4\mathrm{mol\,m^{-3}} \tag{11}$$

the whole Y-H solid solution has transformed into the face-centered cubic β-phase in which all tetrahedral sites are filled with hydrogen atoms. The new phase is known as the dihydride β-$YH_{2\pm x}$ phase in which a further concentration increase leads to the occupation of octahedral sites [27]. At even higher concentrations an yttrium trihydride γ-YH_{3-y} phase starts to precipitate. The phase diagram of the lithium-hydrogen (Li-H) system (see reference [28]) reveals that for the relevant temperatures and for low concentrations of approximately

$$C_{\mathrm{Li}_\alpha} < 0.14\mathrm{at}\% \mathrel{\widehat{=}} 100\mathrm{mol\,m^{-3}} \tag{12}$$

hydrogen isotopes are dissolved as a solute [29] in the liquid lithium (known as the α-phase). At higher concentrations lithium-hydride (LiH) begins to form which precipitates out as solid compounds (known as the α (liq.)+β (sol.) phase) [30].

From the DONES safety regulations we know that the tritium inventory in the lithium loop of DONES will be kept below 0.3g [4]. With a total lithium volume in the loop of approximately $V_{\mathrm{loop}} \approx 10\mathrm{m}^3$, this limit corresponds to a maximum tritium concentration of $C_{\mathrm{Li},^3\mathrm{H,max}} \approx 0.01\mathrm{mol\,m^{-3}}$. The calculated generation rates of ^{1}H, ^{2}H and ^{3}H in the DONES lithium loop reveal that the generation of 0.3g tritium is accompanied by an accumulation of 0.2g hydrogen and 6.7g deuterium in the loop system [31]. Assuming that the hydrogen retention efficiency of the DONES hydrogen hot trap will be similar for all three isotopes we can conservatively estimate that the maximum hydrogen isotope concentration in the loop will be of the order of $C_{\mathrm{Li,H,max}} \approx 0.5\mathrm{mol\,m^{-3}}$ which according to relation (12) stands for a Li-H system in α-phase. For this reason and since the purpose of this work is the development of a model usable as a simulation tool for the design of the hydrogen hot trap of DONES, we consider the Li-H system in our model to be in the state of a low concentration α-phase.

The hydrogen concentration in the yttrium at the pebble surface is defined by a Dirichlet boundary condition. It is specified through the fact that in an infinitesimal area traversing the Y-Li interface the hydrogen solution remains always in chemical equilibrium. This implies an equality of the equilibrium pressures indicated by the pressure-composition-isotherms (PCI) of the Li-H solution and of the Y-H solution [32–34]. For the low concentration region of the α-phase of a metal-hydrogen system the equilibrium pressures are approximately determined by the Sieverts' law [35]

$$C = K_{\mathrm{s}}\cdot\sqrt{P_{\mathrm{eq}}}. \tag{13}$$

Here, K_{s} labels the Sieverts' constant. It quantifies the solubility of hydrogen isotopes in the corresponding metal. Since in this model the considered hydrogen concentration in the lithium is very low, the Sieverts' law should be valid for the Li-H systems. For now we suppose that the establishing hydrogen concentration in the yttrium fulfills relation (10) and assume that the Sieverts' law is valid as well. In this case, the chemical equilibrium at the Y-Li interface can be expressed by

$$P_{\mathrm{eq_{Y-H}}} = P_{\mathrm{eq_{Li-H}}} \iff \left.\frac{C_{\mathrm{Li}}}{K_{\mathrm{s_{Li}}}}\right|_{\mathrm{int}} = \left.\frac{C_{\mathrm{Y}}}{K_{\mathrm{s_Y}}}\right|_{\mathrm{int}}. \tag{14}$$

Also the Sieverts' constant follows an Arrhenius type temperature dependence

$$K_{\mathrm{s}} = K_{\mathrm{s},0}\cdot\exp\left(\frac{E_{\mathrm{s}}}{R_{\mathrm{gas}}T}\right), \tag{15}$$

where $K_{\mathrm{s},0}$ is a pre-exponential factor and E_{s} the enthalpy of formation per dissolved mole of the solution. In several experimental campaigns temperature relations for the Sieverts' constant of hydrogen isotopes in lithium and yttrium could be determined. Depending on the applied experimental methods the different authors report their determined relations in different unit systems. In this work the SI-unit $[\mathrm{mol\,m^{-3}\,Pa^{-\frac{1}{2}}}]$ is used for the Sieverts' constants. The SI-unit of the enthalpy of formation used in this article is $[\mathrm{J\,mol^{-1}\,K^{-1}}]$. For the transition of the reported literature values into SI-units appropriate conversion factors are applied containing the molar mass of yttrium $M_{\mathrm{Y}} = 88.906\mathrm{g\,mol^{-1}}$, the molar mass of lithium $M_{\mathrm{Li}} = 6.94\mathrm{g\,mol^{-1}}$ and the density of yttrium $\rho_{\mathrm{Y}} = 4472\mathrm{kg\,m^{-3}}$. The temperature dependent density of lithium is given by the relation $\rho_{\mathrm{Li}}(T) = 562 - 0.1\cdot T\ [\mathrm{kg\,m^{-3}}]$ [36]. Table 2 presents a list of determined values for $K_{\mathrm{s},0}$ and E_{s} that could be found in literature describing the solubility of

Table 2. Pre-exponential factors $K_{s,0}$ and activation energies E_s of the Sieverts' constant (15) for hydrogen isotopes in yttrium found in the literature. Error margins have not been reported in the literature. Therefore, the considered significant digits of the presented values are assumed from the respective reference taking into account unit conversions. Values printed in bold are those which are chosen to be used for the calculations performed in this work.

	^{1}H in Y	^{2}H in Y	^{3}H in Y	References
$K_{s,0}\left[\frac{\text{mol}}{\text{m}^3}\,\text{Pa}^{-\frac{1}{2}}\right]$	$\mathbf{14.7\times10^{-2}}$	$\mathbf{16.4\times10^{-2}}$	$\mathbf{20.9\times10^{-2}}$	**[37] (Measured)**
	–	–	7.1×10^{-2}	[38] (Measured)
	38.4×10^{-2}	–	–	[37] (Calculated using [33])
	30.7×10^{-2}	–	–	[38] (Calculated using [33])
$E_s\left[\frac{\text{kJ}}{\text{mol K}}\right]$	**97.15**	**95.02**	**90.79**	**[37] (Measured)**
	–	–	95.81	[38] (Measured)
	87.57	–	–	[37] (Calculated using [33])
	89.12	–	–	[38] (Calculated using [33])

Table 3. Pre-exponential factors $K_{s,0}$ and activation energies E_s of the Sieverts' constant (15) for hydrogen isotopes in lithium found in the literature. The temperature dependent density of lithium $\rho_{Li}(T)$ $[\text{kg m}^{-3}]$ arises from the conversion of the literature values of $K_{s,0}$ to SI units. Error margins have not been reported in the literature. Therefore, the considered significant digits of the presented values are assumed from the respective reference taking into account unit conversions. Values printed in bold are those which are chosen to be used for the calculations performed in this work.

	^{1}H in Li	^{2}H in Li	^{3}H in Li	References
$K_{s,0}\left[\frac{\text{mol}}{\text{m}^3}\,\text{Pa}^{-\frac{1}{2}}\right]$	$\mathbf{6.63\times10^{-4}\cdot\rho_{Li}(T)}$	$\mathbf{9.20\times10^{-4}\cdot\rho_{Li}(T)}$	$\mathbf{12.28\times10^{-4}\cdot\rho_{Li}(T)}$	**[39] (Measured)**
	$1.7\times10^{-3}\cdot\rho_{Li}(T)$	–	–	[40] (Measured)
	$6.82\times10^{-4}\cdot\rho_{Li}(T)$	$9.34\times10^{-4}\cdot\rho_{Li}(T)$	–	[41] (Refers to [34, 42])
$E_s\left[\frac{\text{kJ}}{\text{mol K}}\right]$	**51.90**	**46.93**	**42.28**	**[39] (Measured)**
	44.4	–	–	[40] (Measured)
	51.40	46.23	–	[41] (Refers to [34, 42])

hydrogen isotopes in yttrium. In table 3 the same coefficients are shown which were found in literature for hydrogen isotopes dissolved in lithium. When plotted against temperature it is found that the Sieverts' constants $K_{s_{Li}}$ and K_{s_Y} that arise from the presented coefficients in table 2 and table 3 differ merely within one order of magnitude at any given temperature. Therefore, we can assume that the determined values are relatively accurate. For our calculations we make use of the solubility relations for hydrogen isotopes in yttrium which were measured by G.M. Begun *et al* in a high temperature measurement for all three isotopes [37]. Their experimental results are conform with a low temperature solubility measurement of the yttrium-tritium system performed by S.D. Clinton *et al* [38]. Hence, G.M. Begun *et al* concluded that his determined Sieverts' relations seem to be valid in both temperature regions, covering the range 250°C - 1000°C. For the solubility of hydrogen isotopes in liquid lithium this numerical study makes use of the Sieverts' constants which were determined by F.J. Smith *et al* [39] for all three hydrogen isotopes. The temperature dependence of the Sieverts' constant for hydrogen isotopes dissolved in liquid lithium and yttrium is plotted in figure 2. We see that in yttrium as well as in lithium the solubility of hydrogen isotopes decreases with temperature. In yttrium the solubility is several orders of magnitudes higher than in lithium. Their difference even increases towards lower temperatures. At this point we define a new quantity, the partitioning coefficient of the Y-Li system

$$K_{d_{Y-Li}} \equiv \frac{K_{s_Y}}{K_{s_{Li}}}\,. \tag{16}$$

Its value mainly determines how efficient the retention mechanism of hydrogen isotopes from lithium into yttrium will be. Using the chosen Sieverts' relations given in the SI-unit system allows calculating the partitioning coefficients for the corresponding isotopes as done for the creation of figure 3. Substituting equation (16) into relation (14) allows expressing the boundary condition at the Y-Li interface as follows

$$C_Y(r_{peb}, z, t) = K_{d_{Y-Li}} \cdot C_{I,Li}(z, t). \tag{17}$$

Here, $C_{I,Li}(z,t)$ stands for the hydrogen concentration in the lithium close to the pebble boundary layers.

Using equation (17) we calculate the hydrogen concentration in the yttrium that we would find at the pebble interface in case the estimated maximum hydrogen concentration $C_{I,Li} = 0.5\text{mol m}^{-3}$ was present in the lithium. Figure 3 reveals that in the temperature range from 250°C to 325°C the partitioning coefficient lies between $K_{d_{Y-Li}} \approx 4\times10^3$ and $K_{d_{Y-Li}} \approx 2\times10^4$. Hence, we determine a maximum hydrogen concentration

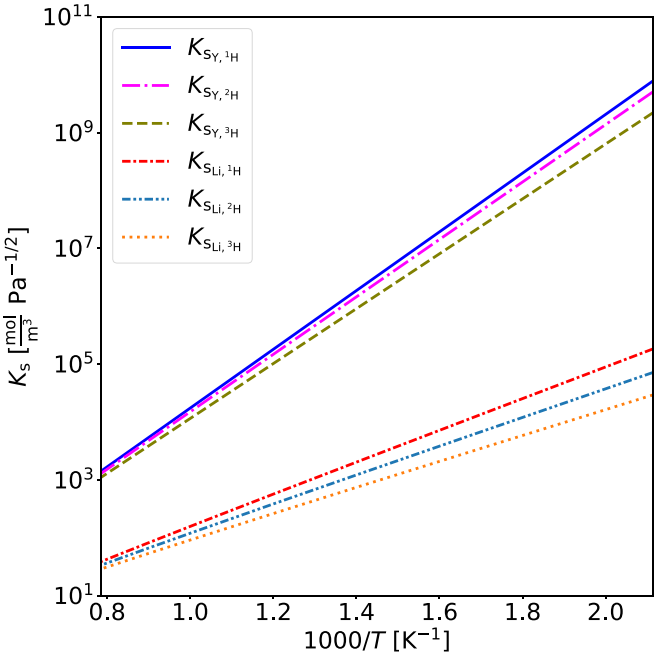

Figure 2. Temperature dependencies of the Sieverts' constants for hydrogen isotopes dissolved in yttrium and lithium measured by G.M. Begun *et al* and F.J. Smith *et al* [37, 39].

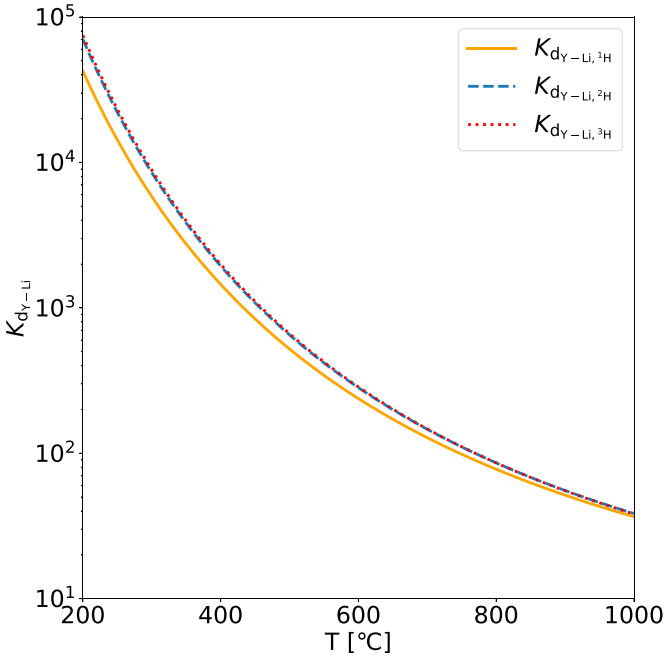

Figure 3. Temperature dependencies of the partitioning coefficients for the yttrium-lithium-hydrogen system calculated using the chosen Sieverts' constant relations presented in figure 2 [37, 39].

in the yttrium of about $C_{Y,H,max} \approx 1 \times 10^4 \text{mol m}^{-3}$ at 250°C. As the Y-H phase diagram and relation (10) indicate, this concentration corresponds to a Y-H system in the α-Y phase with no yttrium dihydrides having formed yet. At higher temperatures even lower concentrations would have established in the yttrium. These findings give confidence to use the Sieverts's law for the calculation of the equilibrium pressures of the Y-H system in equation (14) as it is done in this model.

Studies like [24] or [43] discovered a formation of yttrium dihydrides after an yttrium specimen was exposed to hydrogen loaded liquid lithium. Both experimental works observed the retention process into the yttrium at far higher concentrations in the lithium than those which are considered in this study or expected for the lithium loop of IFMIF/DONES. A formation of the β-$YH_{2\pm x}$ phase would reduce the reliability of the model since at concentrations $C_Y > 1.5 \times 10^4 \text{mol m}^{-3}$ the Sieverts' law is no longer valid for the description of the PCIs. It needed to be replaced by a relation describing the true course of the respective PCIs [37, 44]. In the $\alpha + \beta$ phase transition region at $C_{Y_\alpha} < C_Y < C_{Y_\beta}$ the PCIs of the Y-H system reach a plateau where for an increasing concentration the equilibrium pressures remain almost constant [26, 37]. For the relevant temperature region the plateau or decomposition pressures of the $\alpha + \beta$ phase transition could be theoretically estimated extrapolating Van't Hoff plots of high temperature measurements towards lower temperatures [26]. The relevant decomposition pressures of the $\beta + \gamma$ phase transition in the concentration range $C_Y > C_{Y_\beta}$ have been measured by L.N. Yannopoulos *et al* [33]. Moreover, the effective mobilities of hydrogen isotopes in yttrium at concentrations corresponding to the $\alpha + \beta$ and the $\beta + \gamma$ phase transition are experimentally determined by F.J.A. den Broeder *et al* and could be used as diffusion coefficients for higher concentration regimes [45]. Hence, an extension of the model describing the retention process at concentrations $C_Y > 1.5 \times 10^4 \text{mol m}^{-3}$ is in principle possible but due to the considered concentration limits in IFMIF/DONES not required for this study.

In addition to equation (17) a further boundary condition at the Y-Li interface is given by the equality of particle fluxes on both sides of the interface. Since the hydrogen isotopes are dissolved in atomic form in the liquid metal as well as in the yttrium, neither recombination nor dissociation processes take place at the interface. Hence, only diffusion fluxes are governing the transport across the interface. Due to particle conservation the atomic diffusion flux $J_{MT}(z,t)$ on the lithium side of the interface must be equal to the atomic diffusion flux on the yttrium side of the interface $J_{dif,Y}(r_{peb},z,t)$ and we write

$$J_{dif,Y}(r_{peb},z,t) = J_{MT}(z,t)\,. \tag{18}$$

Both fluxes are oriented contrarily to the positive radial direction of the pebble system and therefore negative. In the following we call J_{MT} the mass transfer diffusion flux of hydrogen isotopes in the liquid lithium at the Y-Li boundary layer. The mass transfer flux is quantified by Fick's first law, meaning it is proportional to the concentration gradient of hydrogen in lithium at the Y-Li interface. However, it would require an extensive numerical three dimensional calculation to determine the exact concentration profile which is present in the lithium flow through the interstitials of a pebble-bed. It is therefore approximated assuming that the lithium flow is sufficiently turbulent to cause a mostly homogeneous concentration C_{Li} in the lithium. Only within a small layer of width d_{BL} around a pebble surface the concentration drastically decreases until it reaches

its lowest value $C_{\mathrm{I,Li}}$ at the Y-Li interface. Figure 4 shows a sketch of the hydrogen concentration distribution in the one dimensional system of an yttrium pebble surrounded by flowing liquid lithium. Using Fick's first law and assuming a linear drop of the hydrogen concentration within the boundary layer of a pebble allows writing a formula for the mass transfer flux on the lithium side of the Y-Li interface

$$J_{\mathrm{MT}}(z,t) = \alpha_{\mathrm{f}} \cdot [C_{\mathrm{I,Li}}(z,t) - C_{\mathrm{Li}}(z,t)]\,, \tag{19}$$

where $\alpha_{\mathrm{f}} = \mathrm{Sh} \cdot D_{\mathrm{Li}}/d_{\mathrm{peb}} \approx D_{\mathrm{Li}}/d_{\mathrm{BL}}$ stands for the mass transfer coefficient and Sh for the Sherwood number. The parameter D_{Li} is the diffusion coefficient of hydrogen isotopes in liquid lithium. Mass transfer between liquids and spheres in packed beds could be investigated by E.J. Wilson and C.J. Geankoplis [46]. Their experimental results allow writing the following two expressions for the mass transfer coefficient applicable in two different Reynolds number regimes [47]

$$\alpha_{\mathrm{f}} = 1.09 \cdot \frac{D_{\mathrm{Li}}}{\epsilon \cdot d_{\mathrm{peb}}} \cdot \mathrm{Re}^{1/3}\mathrm{Sc}^{1/3}\,, \quad 0.001\,6 < \mathrm{Re} < 55 \tag{20}$$

$$\alpha_{\mathrm{f}} = 0.25 \cdot \frac{D_{\mathrm{Li}}}{\epsilon \cdot d_{\mathrm{peb}}} \cdot \mathrm{Re}^{0.69}\mathrm{Sc}^{1/3}\,, \quad 55 < \mathrm{Re} < 1500. \tag{21}$$

For the Reynolds number Re and the Schmidt number Sc we make use of the expressions indicated in [46, 47]

$$\mathrm{Re} = \frac{v_{\mathrm{s}} d_{\mathrm{peb}} \rho_{\mathrm{Li}}}{\eta_{\mathrm{Li}}} \quad \& \quad \mathrm{Sc} = \frac{\eta_{\mathrm{Li}}}{\rho_{\mathrm{Li}} D_{\mathrm{Li}}}, \tag{22}$$

where the superficial velocity of the packed bed is calculated as follows [48]

$$v_{\mathrm{s}} = \frac{\epsilon l_{\mathrm{trap}} F_{\mathrm{Li}}}{V_{\mathrm{Li,trap}}} = \frac{F_{\mathrm{Li}}}{A_{\mathrm{trap}}}. \tag{23}$$

The parameter F_{Li} is the volumetric flow rate through the trap and $V_{\mathrm{Li,trap}} = \epsilon V_{\mathrm{trap}} = \epsilon A_{\mathrm{trap}} l_{\mathrm{trap}}$ the volume occupied by liquid lithium in the interstitial sites between the pebbles. The temperature dependent quantity η_{Li} stands for the dynamic viscosity of liquid lithium. For the calculations performed in this study we make use of the relation [36]

$$\log \eta_{\mathrm{Li}}\,(\pm 19\%) = -3.08 + \frac{58}{T} - 5.2 \times 10^{-4} \cdot T. \tag{24}$$

This equation correlates experimental data presented in [36] with a standard deviation of $\pm 19\%$. Equations (22) and (23) imply that the Reynolds number increases with an increasing flow rate and a decreasing cross section A_{trap} of the trap cylinder. A fully laminar flow in a packed bed can be expected for Reynolds numbers $\mathrm{Re} < 10$ while an entirely turbulent flow is obtained for Reynolds numbers greater than approximately $\mathrm{Re} > 2000$ [48]. Current studies propose an yttrium pebble-bed of $1\mathrm{kg} < m_{\mathrm{Y}} < 50\mathrm{kg}$ for the hydrogen hot trap of DONES [31]. With a conservatively estimated void fraction of $\varepsilon = 0.5$ this would require a trap volume of $0.2\mathrm{l} < V_{\mathrm{trap}} < 10\mathrm{l}$ which is equivalent to a trap cylinder of length $l_{\mathrm{trap}} = 0.5\mathrm{m}$ and diameter $2\mathrm{cm} < d_{\mathrm{trap}} < 16\mathrm{cm}$. The flow rate through the impurity control system of DONES will be of the order of $F_{\mathrm{Li}} \approx 0.5\mathrm{l\,s^{-1}}$. Hence, for the relevant temperatures $250^{\circ}\mathrm{C} < T < 325^{\circ}\mathrm{C}$ we obtain Reynolds numbers in the range $20 < \mathrm{Re} < 1600$ which lie in the partially turbulent flow regime. For this reason, the applied approximation of a mostly homogeneous concentration profile in the lithium flow through the interstitials appears justified within the scope of this study.

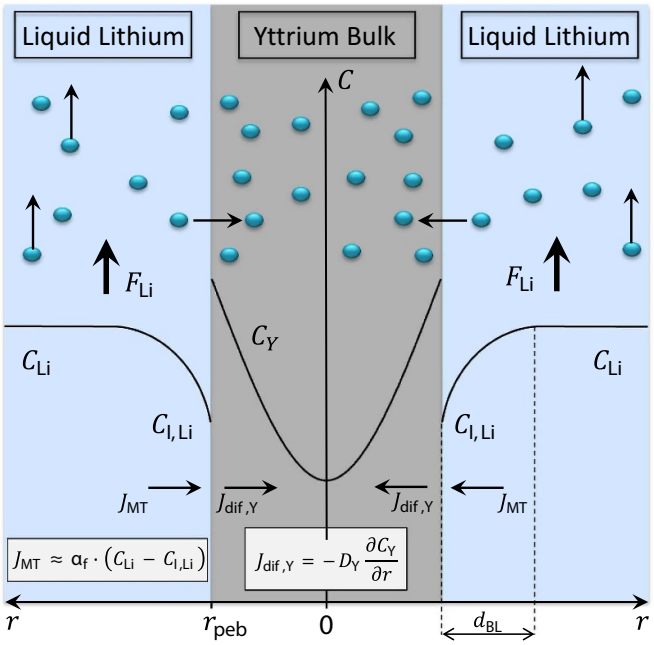

Figure 4. One dimensional system of an yttrium pebble surrounded by flowing liquid lithium showing the governing flux equations and a qualitative snap shot of the time evolving hydrogen concentration distribution in the yttrium bulk and in the liquid lithium.

Table 1 presents a list of different relations for the diffusion coefficient D_{Li} that were found in the literature. All relations were determined in measurements covering different temperature ranges. The deviation of the Arrhenius behavior of the diffusion coefficient of hydrogen in lithium determined by H. Moriyama *et al* and R.E. Buxbaum *et al* arises from the fact that experimental data was fitted against the Stokes-Einstein relation of the diffusion coefficient by making use of an experimentally determined temperature dependence of the dynamic viscosity of liquid lithium [13, 17, 19]. Since this work is focused on system temperatures below 400°C we choose to apply the diffusion relation determined by H. Moriyama *et al* [17]. Its temperature dependence is plotted in figure 1. The plot shows that hydrogen diffuses much quicker in lithium than in yttrium.

As equation (2) reveals, the calculation of the hydrogen isotope retention rate of the yttrium pebbles requires the determination of the retention flux which is equal to the diffusion

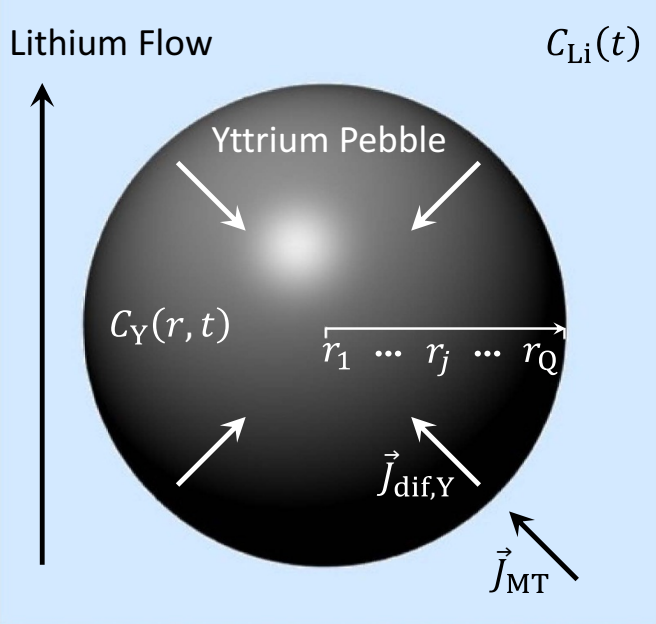

Figure 5. Illustration of the diffusion fluxes from the lithium into an yttrium pebble in two dimensions. In addition, the sketch highlights the applied discretization of the radial direction of a pebble.

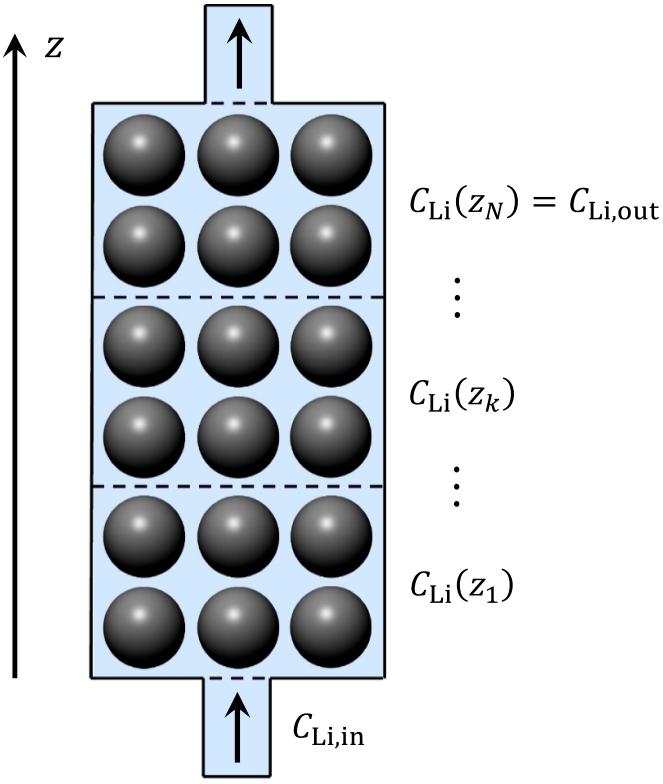

Figure 6. Discretization of the longitudinal z-direction of the cylindrical pebble-bed container.

flux at the surface of the yttrium pebbles. Substituting equation (18) and boundary condition (17) into equation (19) leads to the relation

$$J_{\mathrm{dif,Y}}(r_{\mathrm{peb}},z,t) = \alpha_{\mathrm{f}} \cdot \left[\frac{C_{\mathrm{Y}}(r_{\mathrm{peb}},z,t)}{K_{\mathrm{d_{Y-Li}}}} - C_{\mathrm{Li}}(z,t)\right]. \quad (25)$$

The time evolution of the hydrogen concentration $C_{\mathrm{Li}}(z,t)$ in the liquid lithium that changes along the longitudinal axis of the trap container far away from the Y-Li boundary layer is described using the total time derivative

$$\begin{aligned}\frac{\mathrm{d}C_{\mathrm{Li}}(z,t)}{\mathrm{d}t} &= \frac{\partial C_{\mathrm{Li}}(z,t)}{\partial t} + \frac{\partial C_{\mathrm{Li}}(z,t)}{\partial z}\frac{\partial z}{\partial t} \\ &= \frac{\#_{\mathrm{peb}} \cdot S_{\mathrm{peb}}}{V_{\mathrm{Li}}} \cdot J_{\mathrm{dif,Y}}(r_{\mathrm{peb}},z,t) - \frac{F_{\mathrm{Li}} \cdot l_{\mathrm{trap}}}{V_{\mathrm{Li}}} \cdot \frac{\partial C_{\mathrm{Li}}(z,t)}{\partial z}. \quad (26)\end{aligned}$$

The equations (4), (8), (9), (25) and (26) form a system of coupled differential and algebraic equations. Solving this system would provide the time evolution of $C_{\mathrm{Y}}(r,z,t)$, $C_{\mathrm{Li}}(z,t)$ and $C_{\mathrm{I,Li}}(z,t)$, as well as of the diffusion flux at the interface and in the pebbles $J_{\mathrm{dif,Y}}(r,z,t)$. This would enable calculating the trap efficiency (1) and the total hydrogen isotope retention rate (2) of the pebble-bed.

To solve the presented system of coupled differential equations we choose a numerical finite difference approach. Therefore, the radial direction of each pebble is discretizised into Q discretization nodes $j = 1,\ldots,Q$ with $r_1 = 0\mathrm{m}$, $r_Q = r_{\mathrm{peb}}$, $r_{j+1} = r_j + \Delta r$ and $Q = r_{\mathrm{peb}}/\Delta r + 1$ (see figure 5). The concentrations are determined at the position of the Q discretization nodes $j = 1,\ldots,Q$ while the fluxes are calculated for the $Q-1$ interspaces between the nodes assigned to the radial positions $r_{j=2},\ldots,r_{j=Q}$. Due to boundary condition (9) we write $J_{\mathrm{dif,Y}}(r_{j=1},z_k,t_i) = 0$. The numerical model of the pebble-bed is built on the assumption that in radial direction of the cylindrical trap container the calculated quantities are constant and only vary in the longitudinal z-direction. For the finite difference approach the trap container is segmented using the discretization nodes $z_k = z_1 \ldots z_N$ (see figure 6). The time is discretizised according to $t_{i+1} = t_i + \Delta t$. These definitions allow writing the system of algebraic and differential equations in their finite difference form [49]:

1. Fick's first law (4) describing the diffusion flux in radial direction of a pebble *at* $r_{j=2},\ldots,r_{j=Q}$:

$$J_{\mathrm{dif,Y}}(r_{j+1},z_k,t_i) = -\frac{D_{\mathrm{Y}}}{\Delta r} \cdot [C_{\mathrm{Y}}(r_{j+1},z_k,t_i) - C_{\mathrm{Y}}(r_j,z_k,t_i)] \quad (27)$$

2. Boundary condition (9) providing the concentration for the node $j = 1$ at the center of a pebble. Its numerical finite difference representation can be found in the reference [49]:

$$\begin{aligned}C_{\mathrm{Y}}(r_1,z_k,t_{i+1}) &= C_{\mathrm{Y}}(r_1,z_k,t_i) + \\ &+ \frac{\Delta t \cdot 6D_{\mathrm{Y}}}{\Delta r^2}[C_{\mathrm{Y}}(r_2,z_k,t_i) - C_{\mathrm{Y}}(r_1,z_k,t_i)] \quad (28)\end{aligned}$$

3. Fick's second law (8) describing the time evolution of the concentration profile in radial direction of a pebble for the

nodes $j=2$ to $j=Q-2$:

$$C_{\mathrm{Y}}(r_j,z_k,t_{i+1}) = C_{\mathrm{Y}}(r_j,z_k,t_i) + \frac{D_{\mathrm{Y}}}{j-1}\frac{\Delta t}{\Delta r^2}\cdot \cdot[j\cdot C_{\mathrm{Y}}(r_{j+1},z_k,t_i) - 2(j-1)\cdot C_{\mathrm{Y}}(r_j,z_k,t_i) + +(j-2)\cdot C_{\mathrm{Y}}(r_{j-1},z_k,t_i)] \quad (29)$$

4. Fick's second law (8) expressed by the continuity equation used to describe the time evolution of the concentration in a pebble at the radial position r_{Q-1}:

$$C_{\mathrm{Y}}(r_{Q-1},z_k,t_{i+1}) = C_{\mathrm{Y}}(r_{Q-1},z_k,t_i) - - \frac{\Delta t}{\Delta r}\cdot[J_{\mathrm{dif,Y}}(r_Q,z_k,t_i) - J_{\mathrm{dif,Y}}(r_{Q-1},z_k,t_i)] \quad (30)$$

5. Boundary condition (25) providing the link between the hydrogen concentration in the yttrium and the concentration in the liquid lithium at the Y-Li interface:

$$C_{\mathrm{Y}}(r_Q,z_k,t_i) = K_{\mathrm{d_{Y-Li}}}\cdot\left[C_{\mathrm{Li}}(z_k,t_i) + \frac{J_{\mathrm{dif,Y}}(r_Q,z_k,t_i)}{a_{\mathrm{f}}}\right] \quad (31)$$

6. Total time derivative (26) of the hydrogen concentration in the lithium describing its variation in time and space along the z-axis of the trap:

$$C_{\mathrm{Li}}(z_k,t_{i+1}) = C_{\mathrm{Li}}(z_k,t_i) + \Delta t\cdot\left\{\frac{\#_{\mathrm{peb}}\cdot S_{\mathrm{peb}}}{V_{\mathrm{Li}}}\cdot \cdot J_{\mathrm{dif,Y}}(r_{Q-1},z_k,t_i) - \frac{F_{\mathrm{Li}}\cdot N}{V_{\mathrm{Li}}}\cdot[C_{\mathrm{Li}}(z_k,t_i) - C_{\mathrm{Li}}(z_{k-1},t_i)]\right\} \quad (32)$$

For $k=1$ in the last equation (32) the term $C_{\mathrm{Li}}(z_{k-1},t_i)$ should be replaced by the term $C_{\mathrm{Li,in}}(t_i)$.

Determining the unknown variables of the system of equations in each discretization node requires an equal amount of equations and unknowns. To fulfill this, the initial values of the hydrogen concentrations $C_{\mathrm{Li}}(z_k,t_1)$ and $C_{\mathrm{Y}}(r_j,z_k,t_1)$ in the lithium and in the yttrium need to be known. The input concentration in the lithium at the entrance of the trap $C_{\mathrm{Li,in}} \equiv C_{\mathrm{Li}}(z_1,t_i)$ can be seen as the input parameter of the trap system and hence needs to be given for each instance in time. As an output parameter of the trap system we obtain the concentration $C_{\mathrm{Li,out}} \equiv C_{\mathrm{Li}}(z_N,t_i)$.

For the treatment of the system of equations (27)–(32) the non-causal programming software EcosimPro is used in this work which is capable of solving large systems of coupled differential and algebraic equations [6, 7].

3. Simulation results and discussion

In this section first simulation results are presented which demonstrate the response of the Y-trap model when connecting it to a simplified liquid lithium loop system. We consider a case in which the trap exit is connected with the trap entrance by a pipe of length l_{pipe}. The time and space variation of the hydrogen isotope concentration in the liquid lithium which is flowing through the connecting pipe is described using the total time derivative (26). Therefore, the pipe length is subdivided into U discretization nodes $z_q = z_1,\ldots,z_U$ allowing a finite difference expression of equation (26), written as

$$C_{\mathrm{Li,pipe}}(z_q,t_{i+1}) = C_{\mathrm{Li,pipe}}(z_q,t_i) - \Delta t\cdot \cdot\frac{F_{\mathrm{Li}}\cdot U}{V_{\mathrm{Li}}}\cdot[C_{\mathrm{Li,pipe}}(z_q,t_i) - C_{\mathrm{Li,pipe}}(z_{q-1},t_i)]\,. \quad (33)$$

The fact that no retention flux is present in the tube explains why the first term of equation (32) does not appear in this expression. For a complete numerical description of the new system, consisting of the trap and the pipe, equation (33) needs to be added to the system of equations (27)–(32). The trap and the pipe are linked through the conditions $C_{\mathrm{Li,in}}(t_i) = C_{\mathrm{Li,pipe}}(z_U,t_i)$ and $C_{\mathrm{Li,out}}(t_i) = C_{\mathrm{Li,pipe}}(z_1,t_i)$. Adding these equations to the system finally leads to an equal amount of equations and unknowns making its solution unique. Only the free parameters of the system as well as the initial hydrogen concentration in every discretization point of the different media need to be chosen in advance. In the following, a case study is carried out considering two different scenarios.

3.1. Case A: Finite initial H-isotope concentration

First, we simulate a loop system containing $V_{\mathrm{Li}} = 1\ \mathrm{m}^3$ of liquid lithium heated to $T = 300°\mathrm{C}$. The loop is connected in line with a cylindrical trap container of width $d_{\mathrm{trap}} = 5$ cm which is densely filled with $m_{\mathrm{Y}} = 1\mathrm{kg}$ of $d_{\mathrm{peb}} = 1$ mm yttrium pebbles. The void fraction is assumed to be $\varepsilon = 0.5$ resulting in a trap length of $l_{\mathrm{trap}} = 23$ cm. The volumetric flow rate of the lithium is chosen to be $F_{\mathrm{Li}} = 1\mathrm{l\,s}^{-1}$. The initial hydrogen concentration in the liquid lithium shall be $C_{\mathrm{Li}}(t_0) = 1\mathrm{mol\,m}^{-3}$ for each isotope ^{1}H, ^{2}H and ^{3}H while the yttrium pebbles have no initial hydrogen inventory. The chosen numbers of the spacial discretization nodes are $N=5$, $U=5$ and $Q=101$. The simulation is performed for 4320 time steps of $\Delta t = 10\mathrm{s}$ thus calculating the system behavior for the first 12 h. Using equation (16) and the chosen relations for the Sieverts' constants determined in yttrium and lithium we find the following partitioning coefficients for the different isotopes [37, 39]

$$K_{\mathrm{d_{Y-Li,^1H}}} = 5.8\times10^3, \quad (34)$$

$$K_{\mathrm{d_{Y-Li,^2H}}} = 8.5\times10^3, \quad (35)$$

$$K_{\mathrm{d_{Y-Li,^3H}}} = 8.8\times10^3. \quad (36)$$

In figure 7 the simulated time evolution of the tritium concentration in an yttrium pebble of the first trap segment $z_{k=1}$ is plotted for different moments in time. We see how the particles diffuse towards the center of the pebbles, while particles keep entering into the pebble surfaces. After 12 h the concentration gradients vanish which causes the retention flux to disappear. In figure 8 the average protium, deuterium and tritium concentration in the liquid lithium is plotted against time. We see that the concentrations decrease instantaneously until they finally reach an equilibrium concentration. In chemical

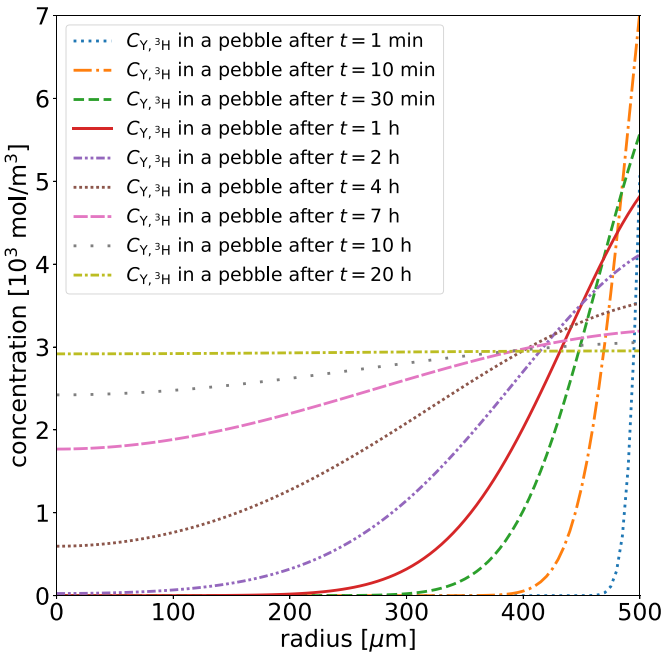

Figure 7. Simulated time evolution of the tritium concentration profile in a pebble of the first segment of the discretisized trap in case of a finite initial tritium concentration in the lithium.

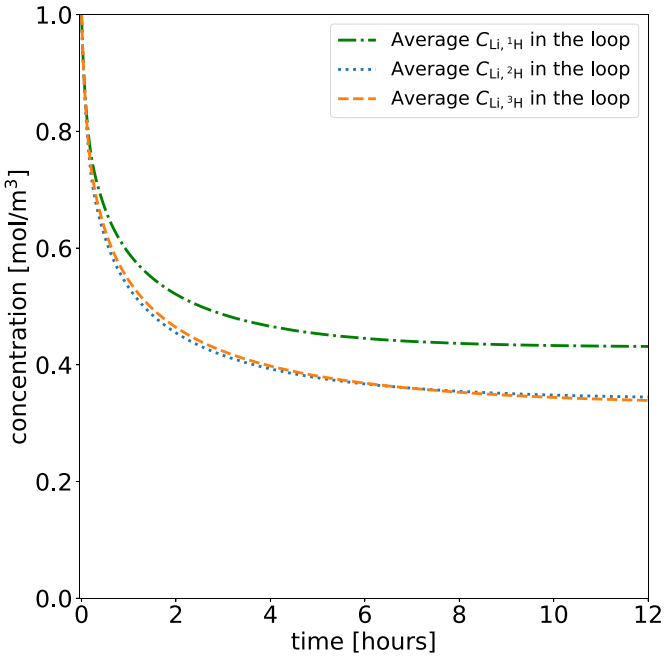

Figure 8. Simulated time evolution of the average hydrogen isotope concentration in 1m^3 of liquid lithium at 300°C flowing through a pebble-bed containing 1 kg of 1 mm yttrium pebbles in case of a finite initial tritium concentration in the lithium.

equilibrium the concentration gradients in the lithium and the yttrium have decreased to zero. The equilibrium concentration establishes when the chemical potential of the hydrogen isotopes in the lithium is equal to that in the yttrium, meaning that $C_Y = K_{d_{Y-Li}} \cdot C_{Li}$ is valid in the whole system. It can be analytically calculated combining this equilibrium condition with the particle conservation relation $n_{Li}(t_0) = n_{Li,eq} + n_{Y,eq}$ which relates the amount of hydrogen atoms in the lithium at $t = 0$s with the distribution of hydrogen atoms in the lithium and the yttrium at equilibrium. We find

$$C_{Li,eq} = \frac{C_{Li}(t_0) \cdot V_{Li}}{V_{Li} + \frac{m_Y}{\rho_Y} \cdot K_{d_{Y-Li}}}. \tag{37}$$

Using this equation we calculate the equilibrium concentration for each isotope and we find $C_{Li,^1H,eq} = 0.43\,\mathrm{mol\,m^{-3}}$, $C_{Li,^2H,eq} = 0.34\,\mathrm{mol\,m^{-3}}$, $C_{Li,^3H,eq} = 0.33\,\mathrm{mol\,m^{-3}}$. As we can see in figure 8 the numerically calculated equilibrium concentrations conform with the concentrations calculated using equation (37).

3.2. Case B: Zero initial concentration & tritium generation

In the following simulation we consider a constant generation of tritium atoms in the liquid lithium flow with a generation rate of $\dot{n}_{gen,^3H} = 1 \times 10^{-8}\,\mathrm{mol\,s^{-1}}$ while the initial concentration of hydrogen isotopes is zero in the lithium as well as in the yttrium. All other parameters are the same as in the previous case. The generation of tritium in the lithium is considered to happen in the first segment $q = 1$ of the tube that connects the input and output of the hydrogen trap. It is introduced in the model by modifying equation (33) adding a generation term only for $q = 1$

$$C_{Li,pipe}(z_1, t_{i+1}) = C_{Li,pipe}(z_1, t_i) + \Delta t \cdot \left\{ \frac{U}{V_{Li}} \cdot \dot{n}_{gen,^3H} - \right.$$
$$\left. - \frac{F_{Li} \cdot U}{V_{Li}} \cdot [C_{Li,pipe}(z_1, t_i) - C_{Li,pipe,in}(t_i)] \right\}. \tag{38}$$

In figure 9 the simulated tritium concentration profile inside of a 1mm wide yttrium pebble is plotted for different instances in time assuming a pebble-bed of mass $m_Y = 1$ kg. Since at the Y-Li interface the chemical equilibrium condition (14) is fulfilled at any time and since we consider a constant tritium generation in the lithium, the tritium concentration at the yttrium surface starts to rise with time. Simultaneously, the tritium moves towards the center of the pebble. We observe that after about seven hours the concentration gradients along the radius seem to not change anymore which results in a constant retention flux. This explains why the concentration in the yttrium rises homogeneously along the radius and almost proportionally with time.

In case no hydrogen trap is connected to the loop the average tritium concentration in the lithium would rise linearly with time as we can see in figure 10 where the average tritium concentration is simulated for the first 24 hours. The other three curves in figure 10 show the tritium concentration in the lithium averaged over the length of the loop if an yttrium pebble-bed is connected to the flow considering a total yttrium mass of either $m_Y = 1$ kg, $m_Y = 2$ kg or $m_Y = 3$ kg. In general we observe that more yttrium pebbles lead to a stronger retention of tritium from the lithium into the pebbles. However, after about seven hours for all three pebble-bed masses the

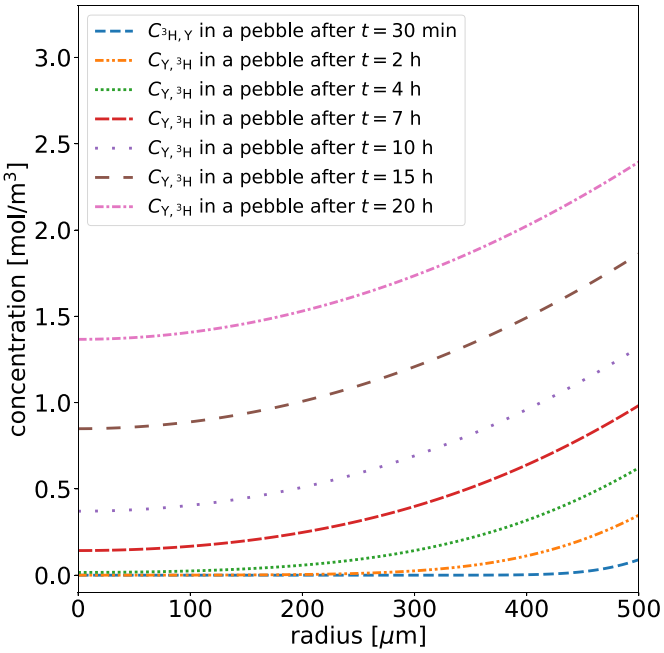

Figure 9. Simulated time evolution of the radial tritium concentration profile in 1mm wide yttrium pebbles that form part of an yttrium pebble-bed of $m_Y = 1$ kg. For this simulation a constant generation of tritium atoms is considered in the liquid lithium.

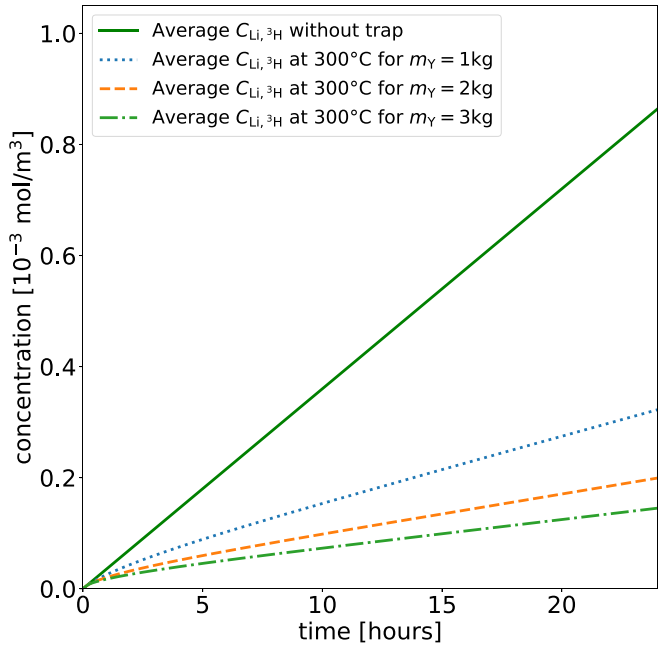

Figure 10. Simulated time evolution of the average tritium concentration in 1 m^3 of liquid lithium considering a constant tritium generation in the loop and different masses of the yttrium pebble-bed.

concentration in the lithium seems to rise linearly and does not approach a steady state in which the generation rate would be equal to the retention rate. It is to mention that in a steady state scenario in which the concentration in the lithium does not rise anymore the pebbles would tend to establish a homogeneous concentration profile causing the retention flux to decrease. This would then move the system out of the steady state causing the concentration in the lithium to rise again. Therefore, it is impossible to reach steady state even for the biggest imaginable pebble-bed. Using more yttrium pebbles only slows down the concentration increase in the liquid lithium. As figure 9 exhibits the retention flux into the pebbles becomes constant after time. As soon as this equilibrium state has been reached for the pebbles in each trap segment we observe that the difference between input and output concentration $C_{\mathrm{Li,in}} - C_{\mathrm{Li,out}}$ of the trap becomes constant as well. In figure 11 the simulated trap efficiency is plotted according to relation (1) considering different masses of the yttrium pebble-bed. We find that as expected for bigger yttrium masses the efficiency is bigger and drops slower than for smaller masses. In figure 12 the average tritium concentration in the lithium is plotted against time considering different lithium temperatures ($T = 250$°C, $T = 300$°C and $T = 350$°C) and a pebble-bed of $m_Y = 1$kg. Although the diffusion coefficient of hydrogen isotopes in lithium and yttrium is smaller for lower temperatures the partitioning coefficient of the yttrium-lithium-hydrogen system drastically increases moving from $T = 350$°C to $T = 250$°C (see figure 3). This explains why in figure 12 tritium is retained more efficiently at lower lithium temperatures.

However, the trap efficiency does not only depend on the yttrium mass and the temperature. The retention flux at the

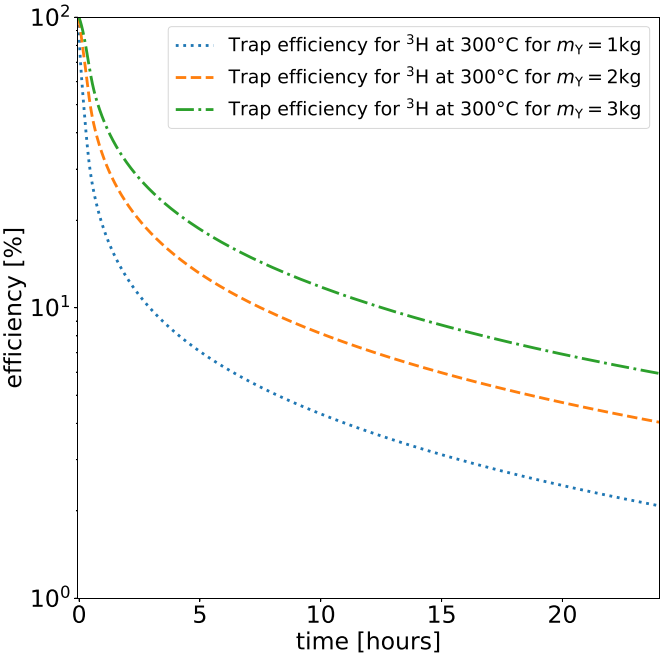

Figure 11. Simulated time evolution of the trap efficiency considering a constant tritium generation in the loop and different pebble-bed masses.

pebble interface exhibits a linear relation with the mass transfer coefficient α_f in equation (25). Beside its dependence on the temperature, the mass transfer coefficient is dependent on the pebble diameter, the trap length and the volumetric flow rate. We find that for higher flow rates as well as for smaller

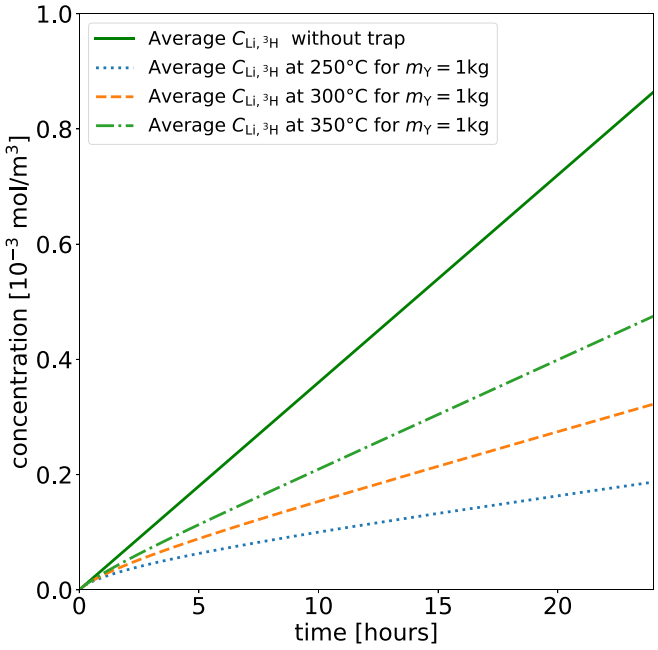

Figure 12. Simulated time evolution of the average tritium concentration in 1 m^3 of liquid lithium considering a constant tritium generation in the loop and different system temperatures.

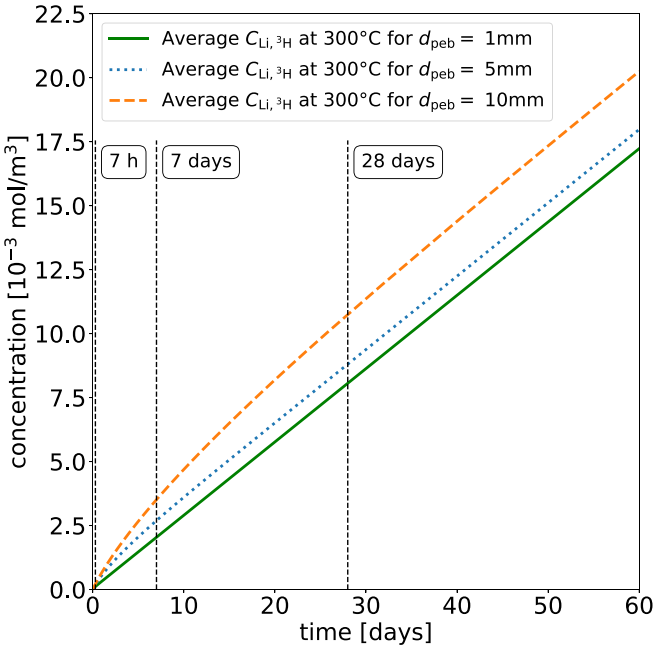

Figure 13. Simulated time evolution of the average tritium concentration in 1m^3 of liquid lithium considering a constant tritium generation in the loop with a pebble-bed of $m_Y = 1$ kg for different yttrium pebble diameters.

yttrium pebbles and narrower trap cylinders, the mass transfer coefficient increases which leads to a higher retention flux. It is to mention that varying these parameters within the same order of magnitude has almost no effect on the retention rate of the trap when considering bigger time scales. Their variation shows its greatest impact on the time after which the trap starts to exhibit its full potential where the retention flux is highest. This state is reached when the concentration gradients along the pebble radii are steepest and reach a constant state in every segment k of the trap. Therefore, the first tritium atoms need to have reached the pebble centre. The required time for this to occur is logically higher for larger pebbles. As visible in figure 9, for pebbles with $d_{peb} = 1$ mm the state of constant concentration gradients in the pebble is reached after about seven hours. Figure 10 shows how this time coincides with the moment the lithium concentration starts to increase linearly and slower than before. In figure 13 the average concentration in the liquid lithium is shown for a pebble-bed of $d_{peb} = 1$ mm, $d_{peb} = 5$ mm and $d_{peb} = 10$mm maintaining all other parameters equal as in the first simulation. For 5mm pebbles the concentration curve exhibits a constant slope after about one week and in case of 10 mm pebbles after about four weeks. The final slope of the concentration increase tends to be the same for different pebble diameters and only depends on the total yttrium mass. A pebble-bed containing smaller yttrium pebbles leads to a final concentration in the lithium which is below the final concentration that establishes in case of bigger pebbles. Hence, a hydrogen trap is most efficient when the lithium is as cold as possible but above its melting point, the mass of the pebble-bed is as high as possible and the pebble diameter is as small as technologically reasonable.

3.3. *Validation of the numerical model*

In order to validate the presented numerical model of a getter pebble-bed the measurement results of a deuterium retention experiment performed in the past by Y. Yamasaki *et al* are simulated [5]. Their experimental system consists of a storage tank where 600 g of molten lithium is charged with deuterium up to a concentration of $C_{Li,^2H}(t_0) = 160\,\text{wppm} \approx 40\ \text{mol}\,\text{m}^{-3}$. Subsequently, it is pumped into a small loop system where its temperature is kept at $T = 300°\text{C}$. In the circuit the liquid lithium is driven by an electromagnetic pump (EMP), thus flowing through a miniature yttrium pebble-bed of length 300 mm which is connected in line with the loop. For the experiment the lithium volumetric flow rate is adjusted to $25\text{ml}\,\text{s}^{-1}$. The trap is filled with 10g of 2–3 mm wide yttrium chips. While the lithium is circulating through the trap the yttrium pebbles absorb the deuterium dissolved in the lithium. During this process lithium samples are extracted at various instances in time and stored in a sample container. After each sample recovery the lithium probe is transferred to an experimental apparatus where the remaining deuterium concentration is measured using the chemical dissolution method [5, 50, 51]. In figure 14 the ratio between the measured concentrations and the initial concentration is plotted against the amount of lithium which has passed through the pebble-bed in the moment when the samples where recovered [5].

The tritium transport into the pebble-bed of this experimental system is numerically simulated using the previously presented model. In its simplified form, the configuration of Y. Yamasaki's experiment is equivalent to the trap-pipe-system which has been numerically treated in subsection 3.1. Only

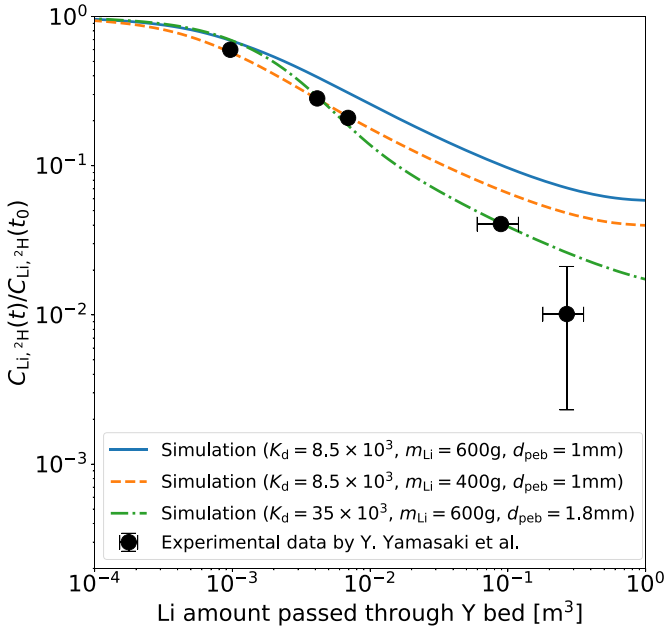

Figure 14. Experimental values of the time evolving concentration ratio $C_{\mathrm{Li},^2\mathrm{H}}(t)/C_{\mathrm{Li},^2\mathrm{H}}(t_0)$ in a deuterium retention experiment performed by Y. Yamasaki *et al* [5]. For validation purposes of the numerical model the experimental results are simulated and compared varying the lithium mass in the loop, the pebble diameter and the partitioning coefficient [5] 2017, adapted by permission of the publisher (Taylor & Francis Ltd, http://www.tandfonline.com).

the system parameters are adjusted to those of the experimental system. As pebble diameter we choose 1 mm since for a fix pebble-bed mass they exhibit the same total surface as 2 mm wide yttrium chips with a thickness of 0.5 mm. For the simulation we consider a 5 mm wide and 28cm long trap container. The assumed void fraction of the pebble-bed is $\varepsilon = 0.6$. In addition to the experimental data points the numerically simulated deuterium concentration ratio is plotted in figure 14 using a continuous line. The first simulation is performed assuming that all 600 g of the molten lithium have entered the lithium loop. We see that the simulated concentration curve almost matches the first experimental data point. Although the simulated curve stays slightly above the measured data it proceeds very close to the second and third data point. As soon as about 100 l have passed the pebble-bed the simulated curve slowly flattens down approaching chemical equilibrium while the experimental values tend to drop even stronger than ever before reaching concentration ratios of $C_{\mathrm{Li},^2\mathrm{H}}/C_{\mathrm{Li},^2\mathrm{H}}(t_0) \approx (10 \pm 9) \times 10^{-3}$. However, calculating the equilibrium concentration in the lithium using equation (37) reveals a minimum possible concentration ratio of $C_{\mathrm{Li},^2\mathrm{H,eq}}/C_{\mathrm{Li},^2\mathrm{H}}(t_0) = 5.9 \times 10^{-2}$ which is conform with the behavior of the simulated concentration ratio. Hence, not the model itself but another factor seems to be responsible for the inconsistency between experiment and simulation.

For the verification of the numerical model it needs to be taken into account that important information about the exact set-up of the experiment, its dimensions and its execution was not available and could therefore not be considered in the model with sufficient detail. Without the missing information an exact numerical reproduction of the experimental results is not possible. For example, the amount of lithium that was eventually in contact with the pebble-bed is unknown since only the total mass of molten lithium in the lithium storage tank has been reported in the reference article. The loop is filled by pressurizing the space above the lithium surface in the storage tank with argon gas. As a result the lithium rises up through a thin pipe filling the loop system with liquid lithium while the lithium surface sinks down. The pipe inlet is located at the bottom of the storage tank. As soon as the sinking lithium surface reaches the pipe inlet the filling process stops. This implies that some of the lithium will remain in the storage tank. Therefore, it is a very probable scenario that eventually less than 600 g of liquid lithium have entered the loop. In order to observe the influence of this scenario on the simulation results, the simulation is repeated assuming that only 400 g of lithium have entered the loop. We see that the simulated curve now matches the first three experimentally determined values (see dashed line in figure 14). However, the curve proceeds above the last two data points while approaching chemical equilibrium. During the hydrogen retention process it is reasonable to assume that a not negligible amount of deuterium has diffused into the loop walls. This could explain why the last measured deuterium concentration value is smaller than the simulated concentrations at equilibrium.

The value of the equilibrium concentration is mainly determined by the partitioning coefficient $K_{\mathrm{d}_{\mathrm{Y-Li},^2\mathrm{H}}}$. For the previous simulations the value $K_{\mathrm{d}_{\mathrm{Y-Li},^2\mathrm{H}}} = 8.5 \times 10^3$ has been used after being calculated as the ratio of the Sieverts' constants of deuterium in yttrium and lithium at $T = 300°\mathrm{C}$ reported by G.M. Begun *et al* and F.J. Smith *et al* [37, 39]. To study the sensitivity of the simulation outcome to the value of the partitioning coefficient which was used for the numerical model we study a case assuming the partitioning coefficient was underestimated and $K_{\mathrm{d}_{\mathrm{Y-Li},^2\mathrm{H}}} = 35 \times 10^3$ instead. Moreover, we assume that all 600g of the molten lithium have entered the loop and choose a pebble diameter of 1.8 mm. Such pebbles exhibit the same total surface as 3mm wide yttrium chips with a thickness of 1 mm. The dash-dotted line in figure 14 shows the resulting curve of the simulated concentration decrease in the liquid lithium. We see that the overall match between experimental data and simulation results significantly improves. This gives rise to the assumption that not precisely measured Sieverts' constants could have resulted in an incorrectly calculated partitioning coefficient. This could explain the mismatch between simulation and experimental results.

Another reason for the faster decreasing experimentally determined concentrations in comparison with the simulation results might originate from a formation of yttrium dihydrides on the surface of the yttrium chips. This is a probable scenario, since the initial hydrogen concentration in the lithium is relatively high. Applying the Sieverts' law for the Li-H system at $T = 300°\mathrm{C}$ with $C_{\mathrm{Li},^2\mathrm{H}}(t_0) \approx 40\ \mathrm{mol\,m^{-3}}$ yields an equilibrium pressure of about $P_{\mathrm{eq}} \approx 2 \times 10^{-5}$ Pa . As indicated by relation (14) at the interface of the Y-Li and the Li-H system the equilibrium pressures are equal. For the Y-H

system at 300°C K. Hiyane *et al* estimated a decomposition pressure of the $\alpha+\beta$ phase transition to be of the order of $P = 1 \times 10^{-8}$ Pa [50]. For the $\beta+\gamma$ phase transition L.N. Yannopoulos *et al* measured a decomposition pressure of about $P = 6 \times 10^{3}$ Pa [26, 33]. Since the calculated equilibrium pressure of the Y-Li-H system lies between the two decomposition pressures the yttrium chips in the experiment probably transformed to the dihydride β-$YH_{2\pm x}$ phase after being put in contact with the lithium. Since the developed model is based on the assumption that all observed metal-hydrogen systems are present in α-Y phase where the Sieverts' law can be applied it should be expected that simulating the presence of such high concentrations in the lithium is accompanied by a reduction of the reliability of the model. The finding that Y. Yamasaki *et al* observed a more efficient deuterium retention than predicted with our model can be considered as an indicator for the predication that a formation of yttrium dihydrides results in an acceleration of the gettering process of hydrogen isotopes from lithium into the yttrium. This could be explained by the fact that in the $\alpha+\beta$ phase transitions the Sieverts' law is no longer valid and the PCIs of the Y-Li system reach a plateau. Hence, a slight concentration increase in the lithium would cause an abrupt and strong rise of the concentration at the surface of the yttrium bulk [45]. This leads to a sudden rise of the concentration gradients in the yttrium and thus to bigger retention fluxes. Therefore, at concentrations greater than those considered in the lithium loops of IFMIF/DONES the model probably starts underestimating the efficiency of the trap. However, even for higher concentrations the numerical model would still remain a tool capable of simulating the minimum expected retention rate of any given yttrium pebble-bed. For this reason, the model enables a reliable and safe design of a hydrogen hot trap for IFMIF/DONES.

In general, it is difficult to validate the accuracy of the numerical model as long as the correctness of the single experimental parameters and especially the partitioning coefficient are not confirmed with sufficient certainty. Nevertheless, the model allows producing simulation results which are satisfyingly close to the experimental data. If the model had been used to reproduce results of a retention experiment that works with hydrogen concentrations in the range of those which are considered for IFMIF/DONES, the simulation and experimental data would have probably matched even more.

4. Conclusion

In the presented work a numerical model has been developed from scratch capable of describing the hydrogen transport from flowing liquid metal into a getter pebble-bed. Especially the hydrogen retention from flowing liquid lithium by yttrium pebbles has been considered. The model focuses on solving the transport equations of the system taking into account the boundary conditions at the interfaces of the different media. The considered boundary conditions are based on the assumption that the Li-H system as well as the Y-H system are present in their α-phases. The model depends on the correctness of several experimental parameters that were determined in the past by different experimental campaigns.

In a case study first simulation results are analyzed. Therefore, a system is considered in which the inlet and the outlet of the trap is connected by a simple pipe. First, a scenario is simulated in which the lithium contained in the trap and the pipe has a finite initial hydrogen isotope concentration while the initial concentration in the yttrium is zero. The shape of the concentration decrease in the lithium behaves as expected reaching chemical equilibrium after a steep initial concentration drop. We find that the trap is most efficient for tritium, then deuterium and then protium. Furthermore, a case is considered in which the initial concentrations are zero and tritium is generated in a constant manner. It is discovered that for higher yttrium masses the concentration increase in the loop is slowed down more efficiently but never reaches a stationary state in which the absorption flux would be equal to the generation rate. Although after time the retention rate of the trap reaches a constant value the trap efficiency decreases very quickly. Moreover, lower lithium temperatures significantly improve the trap efficiently in the temperature region of interest. A variation of all other free system parameters have a minor impact on the trap behavior.

In order to validate the reliability of the trap model experimental data of a measurement performed by Y. Yamasaki *et al* is reproduced in a numerical simulation. In their experiment deuterium loaded liquid lithium is flowing through a miniature yttrium pebble-bed. As a result the deuterium concentration in the lithium decreases which was measured at various points in time. For the numerical reproduction of the experimental results the boundary variables and the initial conditions of the experimental set-up are considered as input parameters of the simulation. We find that the simulated concentration evolves very similar to the experimental values. However, the simulated concentration drop is slightly flatter leading to a growing difference between experimental and simulation results. This small systematic difference can probably be attributed to the fact that important information about the exact conditions and geometry of the experiment was not available. Simulating the same experiment considering a higher partitioning coefficient significantly improved the match between simulation and experimental results. This finding supports the assumption that the Sieverts' constants for hydrogen in yttrium and lithium used in the model were measured with insufficient accuracy. Moreover, due to a relatively high concentration of hydrogen isotopes in the lithium a formation of yttrium dihydrides is probable and would have made the model less reliable for the numerical reproduction of the experimental data. Therefore, a better correspondence between simulated and experimental results can not be expected.

For a more accurate and meaningful validation of the model another hydrogen retention experiment should be constructed and executed on site containing a lithium loop connected to an yttrium pebble-bed. Thus, all necessary input parameters would be directly available with sufficient detail and the presence of lower hydrogen concentrations could be experimentally observed. For the future, an extension of the numerical model is foreseen which aims to accurately simulate the

retention behavior of an yttrium pebble-bed at higher concentration regimes taking into account the formation of yttrium di- and trihydrides. As a final remark, we can say that the developed numerical model forms a trustful tool to simulate the hydrogen retention process from flowing liquid lithium into an yttrium pebble-bed.

Acknowledgments

This work has been carried out within the framework of the EUROfusion Consortium and has received funding from the Euratom research and training programme 2014-2018 and 2019-2020 under Grant Agreement No. 633053. The views and opinions expressed herein do not necessarily reflect those of the European Commission.

This work has been partially funded by the MINECO Ministry under project ENE2013-43650-R. S.J. Hendricks acknowledges a pre-PhD contract of the Spanish MICINN.

ORCID iDs

S.J. Hendricks https://orcid.org/0000-0002-9784-487X
E. Carella https://orcid.org/0000-0002-4802-2546
C. Moreno https://orcid.org/0000-0003-1497-5119
J. Molla https://orcid.org/0000-0001-5407-1611

References

[1] Ibarra A. *et al* 2019 The european approach to the fusion-like neutron source: the IFMIF-DONES project *Nucl. Fusion* **59** 46–56
[2] Nitti F. *et al* 2015 The design status of the liquid lithium target facility of IFMIF at the end of the engineering design activities *Fusion Eng. Des.* **100** 425–30
[3] Aiello A. 2019 Engineering design of a prototypical lithium purification loop Technical report, EUROfusion, EFDA_D_2N29VE
[4] Chacon R.R. 2018 Presentation ENS Project. 11th Design Configuration and Interfaces meeting EUROfusion, 2MLY4U
[5] Yamasaki Y., Fukada S., Hiyane K. and Katayama K. 2017 Study on transfer behavior of hydrogen isotopes from fluidized Li to Y for Li blanket *Fusion Sci. Technol.* **71** 501–6
[6] Vázquez F., Jiménez J. and Garrido J. 2010 *Introduction to Modelling and Simulation With Ecosimpro* (Madrid: Pearson)
[7] Carella E. and Moreno C. 2015 Fuel cycle simulator development *Final report* EUROfusion, EFDA_D_2L3JCZ
[8] Wert C. and Zener C. 1949 Interstitial atomic diffusion coefficients *Phys. Rev.* **76** 1169–75
[9] Molla J. 2018 Baseline for the design of H trap *Technical report* EUROfusion, EFDA_D_2N4LSS
[10] Talbot J.B., Clinton S.D. 1979 Liquid lithium blanket processing studies *8th Symp. on Engineering Problems of Fusion Research* (San Francisco, CA, 13–16 November 1979) pp 278–85 (https://inis.iaea.org/search/search.aspx?orig_q=RN:11519449)
[11] Vorobyov V.V. and Ryabchikov L.N. 1966 p 7 Diffusion of hydrogen in yttrium *Report* 14 (ORNL-TR–4968)
[12] Fisher P.W. and Tanase M. 1984 Diffusivities of hydrogen in yttrium and yttrium alloys *J. Nucl. Mater.* **123** 1536–40
[13] Buxbaum R.E. and Johnson E.F. 1985 Diffusivity of hydrogen isotopes in liquid lithium and in solid yttrium *Industrial Eng. Chem. Fundamentals* **24** 180–2
[14] Carlson O.N. and Schmidt F.A. 1966 Electrotransport of interstitial atoms in yttrium *J. Less Common Metals* **10** 1–11
[15] Frisius F., Lahann H.J., Mertins H., Spalthoff W. and Wille P. 1972 On the isothermal hydrogen diffusion in zircaloy-yttrium combinations *Berichte der Bunsengesellschaft für physikalische Chemie* **76** 824–5
[16] Frisius F., Hackbarth H. and Wille P. 1976 Experiments on the diffusion of hydrogen in yttrium *Atomkernenergie* **27** 287–8
[17] Moriyama H., Iwasaki K. and Ito Y. 1992 Transport of tritium in liquid lithium *J. Nucl. Mater.* **191-194** 190–3
[18] Alire R.M. 1976 Transport of hydrogen in liquid lithium *J. Chem. Phys.* **65** 1134–7
[19] Shpil'rain E.E., Soldatenko Y.A., Yakimovich V.A., Fomin V.A., Savchenko V.A., Belova A.M., Kagan D.N. and Dvaniova I.F. 1965 Experimental investigation of thermal and electrical properties of liquid alkali metals at high temperatures *High Temperature* **3** 870–4
[20] Fukada S., Kinoshita M., Kuroki K. and Muroga T. 2005 Hydrogen diffusion in liquid lithium from 500°C to 650°C *J. Nucl. Mater.* **346** 293–7
[21] Völkl J. and Alefeld G. 1975 Hydrogen diffusion in metals *Diffusion in Solids* ed A.S. Nowick and J.J. Burton (Amsterdam: Elsevier)
[22] Edao Y., Fukada S., Yamaguchi S., Wu Y. and Nakamura H. 2010 Tritium removal by Y hot trap for purification of IFMIF Li target *Fusion Eng. Des.* **85** 53–7
[23] Beaudry B.J. and Spedding F.H. 1975 The solubility of RH^{2-x} in Gd, Er, Tm, Lu and Y from ambient to 850°C *Metall. Trans.* B **6** 419–27
[24] Buxbaum R.E. and Johnson E.F. 1980 The use of yttrium for the recovery of tritium from lithium at low concentrations *Nucl. Technol.* **49** 307–14
[25] Khatamian D. and Manchester F.D. 1988 The H-Y (hydrogen-yttrium) system *Bull. Alloy Phase Diagrams* **9** 252–60
[26] Fu K., Jiang X., Guo Y., Li S., Zheng J., Tian W. and Li X. 2018 Experimental investigation and thermodynamic assessment of the yttrium-hydrogen binary system *Progress Natural Sci.: Mater. Int.* **28** 332–6
[27] Remhof A. 1999 *Hydrogen in yttrium films: structure and phase formation* PhD thesis Ruhr-Universität Bochum (https://inis.iaea.org/search/search.aspx?orig_q=RN:33019574).
[28] Adams P.F., Down M.G., Hubberstey P. and Pulham R.J. 1975 Solubilities and solution and solvation enthalpies, for nitrogen and hydrogen in liquid lithium *J. Less Common Metals* **42** 325–34
[29] Christenson M., Panici D., Moynihan C., Wendeborn J., Anderson J. and Ruzic D. 2019 A study on hydrogen absorption and dissolution in liquid lithium *Nucl. Fusion* **59** 026011
[30] Mueller W.M., Blackledge J.P. and Libowitz G.G. 1968 *Metal Hydrides* (New York and London: Academic)
[31] Moreno C., Hendricks S.J. and Molla J. 2020 Update of the evaluation of tritium production and permeation in the loop *Technical report*, EUROfusion, EFDA_D_2NQB2S
[32] Fukai Y. 2005 *The Metal-Hydrogen System* (Berlin Heidelberg: Springer)
[33] Yannopoulos L.N., Edwards R.K. and Wahlbeck P.G. 1965 The thermodynamics of the yttrium-hydrogen system *J. Phys. Chem.* **69** 2510–15
[34] Veleckis E., Van Deventer E.H. and Blander M. 1974 Lithium-lithium hydride system *J. Phys. Chem.* **78** 1933–40

[35] Sieverts A. 1929 The absorption of gases by metals *Zeitschrift für Metallkunde* **21** 37–46
[36] Davison H.W. 1968 Compilation of thermophysical properties of liquid lithium *Tech. Rep.* NASA Lewis Research Center
[37] Begun G.M., Land J.F. and Bell J.T. 1980 High temperature equilibrium measurements of the yttrium–hydrogen isotope (H2, D2, T2) systems. *J. Chem. Phys.* **72** 2959–66
[38] Clinton S.D. and Watson J.S. 1979 The solubility of tritium in yttrium at temperatures from 250 to 400°C *J. Less Common Metals* **66** 51–7
[39] Smith F.J., Land J.F., Begun G.M. and La Gamma de Batistoni A.M. 1979 The solubility and isotopic exchange equilibrium for hydrogen isotopes in lithium *J. Inorg. Nucl. Chem.* **41** 1001–9
[40] Katsuta H., Ishigai T. and Furukawa K. 1977 Equilibrium pressure and solubility of hydrogen in liquid lithium *Nucl. Technol.* **32** 297–303
[41] Veleckis E., Van Deventer E.H. and Blander M. 1979 Decomposition pressures in the $(\alpha + \beta)$ fields of the Li-LiH, Li-LiD and Li-LiT systems *J. Nucl. Mater.* **79** 20–7
[42] Veleckis E. 1977 Thermodynamics of the lithium-lithium deuteride system *J. Phys. Chem.* **81** 526–31
[43] Hubberstey P., Adams P.F., Pulham R.J., Down M.G. and Thunder A.E. 1976 Hydrogen in liquid alkali metals *J. Less Common Metals* **49** 253–69
[44] Lässer R. 1989 *Tritium and Helium-3 in Metals* (Berlin Heidelberg: Springer)
[45] den Broeder F.J.A. *et al* 1998 Visualization of hydrogen migration in solids using switchable mirrors *Nature* **394** 656–8
[46] Wilson E.J. and Geankoplis C.J. 1966 Liquid mass transfer at very low reynolds numbers in packed beds *Industrial Eng. Chem. Fundamentals* **5** 9–14
[47] Takeda T., Ying A. and Abdou M.A. 1995 Analysis of tritium extraction from liquid lithium by permeation window and solid gettering processes *Fusion Eng. Des.* **28** 278–85
[48] Rhodes M. 2008 *Introduction to Particle Technology* (New York: Wiley)
[49] Crank J. 1975 *The Mathematics of Diffusion* (Oxford: Oxford University Press)
[50] Hiyane K., Fukada S. and Yamasaki Y. 2016 Removal of low-concentration deuterium from fluidized Li loop for IFMIF *Fusion Eng. Des.* **109-111** 1340–4
[51] Esaki K., Hiyane K., Fukada S., Wakai E., Ito Y., Nitti F.F. and JAEA IFMIF group 2015 Study on control of non-metallic impurities in liquid lithium *J. Plasma Fusion Res.* **11** 36–40